A case study on seismic behavior of rectangular tanks considering fluid - structure interaction

K. Kotrasova and E. Kormanikova

***Abstract*—**Liquid-storage tanks are used to store a variety of liquids. The fluid develops impulsive and convective action on liquid storage rectangular container during earthquake. This paper provides the theoretical background for specification of hydrodynamic effect of fluid on solid of tank fixed to rigid foundation and numerical solution for Finite Element Method (FEM), Arbitrary Lagrangian Eulerian (ALE), Fluid Structure Interactions (FSI) formulation. FEM ALE FSI formulation was used for numerical model of seismic response of tank - the endlessly long shipping concrete channel. The accelerogram Loma Prieta was considered as horizontal ground motion.

***Keywords* —** tank, fluid, earthquake, finite element method arbitrary Lagrangian-Eulerian formulation, fluid-structure interaction

I. Introduction

The earthquake isn't direct risk for humans and environment, but ground motion effect causes long-range damages on buildings, up to their collapse. It caused wide-ranging consequences in rebuilding and makes it difficult to return to a normal functioning of society. Large damages are caused far away from the epicenter of the seismic waves too. Financial losses, as a result of earthquakes, have grown continuously over the last years. It isn't due to an increase in earthquake intensity and frequency of earthquakes, but due to growing financial value of building materials. The economic value of containers with tank's filling isn't decisive, but damages of the storage buildings always produce high danger to human health, infrastructure and environment.

Liquid-storage rectangular tanks are used to store a variety of liquids. Storage tanks hold toxic liquids too, such as petroleum, oil, liquefied natural gas, chemical fluids, and different forms of wastes. Therefore, this type of structures must show satisfactory performance, especially, during earthquakes.

Due to these reasons, this type of structures which are special in construction and in function from engineering point of view must be constructed well to be resistant against earthquakes. There have been numerous studies done for dynamic behavior of fluid containers; most of them are concerned with cylindrical tanks. But very few studies on the dynamic response of rectangular containers exist.

The seismic analysis and design of liquid storage tanks is, due to the high complexity of the problem, in fact, really complicated task. Number of particular problems should be taken into consideration, for example: dynamic interaction between contained fluid and tank, sloshing motion of the contained fluid; and dynamic interaction between tank and sub-soil. Those belong to wide range of so called Fluid Structure Interactions (FSI).

As known from very upsetting experiences, liquid storage tanks have collapsed or heavily damaged during earthquakes all over the world. Damage or collapse of the tanks causes some unwanted events such as shortage of drinking and utilizing water, uncontrolled fires and spillage of dangerous fluids. Even uncontrolled fires and spillage of dangerous fluid subsequent to a major earthquake may cause substantially more damage than the earthquake itself.

Knowledge of seismic effect acting on solid domain of containers during an earthquake is important for good design of earthquake resistance structure/facility - tanks, made from steel, concrete or different material. The knowledge of forces, pressures acting onto walls and the bottom of containers, pressures in solid of tanks, liquid surface sloshing process and maximal height of liquid's wave during an earthquake, plays essential role in reliable and durable design of earthquake resistance structure/facility - containers. The analysis of a coupled multi-physics system is frequently required today to understand the behavior of the system. In particular, the analysis of problems that involve fluid flows interacting with solids or structures is increasingly needed in diverse applications including ground-supported tanks used to store a variety of liquids [5,10,19].

II. Mechanical model

The dynamic analysis of a liquid - filled tank may be carried out using the concept of generalized single - degree - of freedom (SDOF) systems representing the impulsive and convective modes of vibration of the tank - liquid system as shown in Fig. 1. For practical applications, only the first convective modes of vibration need to be considered in the analysis of mechanical model. The impulsive mass of liquid m_i is rigidly attached to tank wall at height h_i. Similarly

Kamila Kotrasova is with the Department of Structural Mechanics, Institute of Structural Engineering, The Technical University of Kosice, Faculty of Civil Engineering, Vysokoskolska 4, 042 00 Kosice, Slovak Republic (corresponding author to provide phone: +421 55 6024294; e-mail: kamila.kotrasova@tuke.sk).

Eva Kormanikova is with the Department of Structural Mechanics, Institute of Structural Engineering, The Technical University of Kosice, Faculty of Civil Engineering, Vysokoskolska 4, 042 00 Kosice, Slovak Republic (e-mail: eva.kormanikova@tuke.sk).

convective mass m_{cn} is attached to the tank wall at height h_{cn} by a spring of stiffness k_{cn}. The mass, height and natural period of each SDOF system are obtained by the methods described in [30],

$$m_i = m2\gamma\sum_{n=0}^{\infty}\frac{I_1(\nu_n/\gamma)}{\nu_n^3 I_1^{'}(\nu_n/\gamma)}, \quad (1)$$

$$h_i = H\frac{\sum_{n=0}^{\infty}\frac{(-1)^n I_1(\nu_n/\gamma)}{\nu_n^4 I_1^{'}(\nu_n/\gamma)}\left(\nu_n(-1)^n-1\right)}{\sum_{n=0}^{\infty}\frac{I_1(\nu_n/\gamma)}{\nu_n^3 I_1^{'}(\nu_n/\gamma)}}, \quad (2)$$

$$m_{cn} = m\frac{2\tanh(\lambda_n\gamma)}{(\lambda_n\gamma)(\lambda_n^2-1)}, \quad (3)$$

$$h_{cn} = H\left(1+\frac{1-\cosh(\lambda_n\gamma)}{(\lambda_n\gamma)\cdot\sinh(\lambda_n\gamma)}\right), \quad (4)$$

$$k_{cn} = \omega_{cn}^2 m_{cn} \quad (5)$$

$$\omega_{cn}^2 = g\frac{\lambda_n}{L}\tanh(\lambda_n\gamma) \quad (6)$$

where $\nu_n = \pi\frac{2n+1}{2}$, $\gamma = H/L$, $I_1(\cdot)$ and $I_1^{'}(\cdot)$ denote the modified Bessel function of order 1 and its derivate. The derivate can be expressed in terms of the modified Bessel functions of order 0 and 1 as $I_1^{'}(x) = \frac{dI_1(x)}{dx} = I_0(x) - \frac{I_1(x)}{x}$.

λ_n are solution of Bessel function of first order, λ_1=1.8412; λ_2=5.3314; λ_3=8.5363, λ_4=11.71, λ_5=14.66 and $\lambda_{5+i}=\lambda_5+5\ i$ (i=1,2,...)).

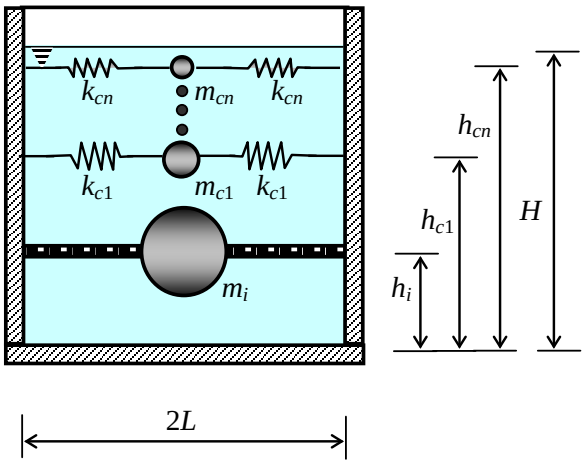

Fig. 1 liquid-filled tank modelled by generalized single degree of freedom systems

For a horizontal earthquake ground motion, the response of various SDOF systems may be calculated independently and then combined to give the base shear and overturning moment. The most tanks have slenderness ratio of tank γ, whereby 0.3 < γ < 3. Tank's slimness is given by relation $\gamma = H/L$, where H is the filling height of fluid in the tank and 2L is inside width of tank.

III. FEM - Fluid-structure interaction

The finite element method is well established for the analysis of complex engineering problems involving structures, fluids and fluid structure interaction. The fluid structure interaction problem is presented in various engineering activities, as civil buildings, mechanical devices, biomechanics etc. The interaction between fluids and structures can, in many practical engineering problems, significantly affect the response of the structure and hence needs to be properly taken into account in the analysis.

A. Problem formulation

For the fluid-structure interaction analysis, there are possible three different finite element approaches to represent fluid motion - Eulerian, Lagrangian and mixed methods. In the Eulerian approach, velocity potential (or pressure) is used to describe the behavior of the fluid, whereas the displacement field is used in the Lagrangian approach. In the mixed approaches, both the pressure and displacement fields are included in the element formulation [1,9].

In fluid-structure interaction analyses, fluid forces are applied into the solid and the solid deformation changes the fluid domain. For most interaction problems, the computational domain is divided into the fluid domain and solid domain, where a fluid model and a solid model are defined respectively, through their material data, boundary conditions, etc. The interaction occurs along the interface of the two domains. Having the two models coupled, we can perform simulations and predictions of many physical phenomena [6,11].

In many fluid flow calculations, the computational domain remains unchanged in time. Such the problems involve rigid boundaries and are suitable handled in Eulerian formulation of equilibrium equations [2,12-17]. In the case where the shape of the fluid domain is expected to change significantly, modified formulation called Arbitrary Lagrangian-Eulerian (ALE) formulation was adopted to simulate the physical behavior of the domain of interest properly. The ALE description is designed to follow the boundary motions rather than the fluid particles. Thus, the fluid particles flow through a moving FE-mesh. Basically there are two different algorithms available for generation of possible moving mesh:

- remeshing of fluid domain, which is computationally expensive procedure,
- rezoning of FE-mesh of fluid domain. This procedure is quite fast while precise enough if no dramatic changes of fluid domain is expected.

B. Structural Equations

The Lagrangian equations of motion of the structure are

$$\rho\frac{\partial^2\mathbf{u}}{\partial t^2} = \nabla\cdot\tau + \mathbf{f}^B, \quad (7)$$

where ρ is the density, $\mathbf{u}$ is the vector of structural displacements, t is the time, τ is the Cauchy stress tensor, $\mathbf{f}^B$ is

the vector of body forces and $(\nabla\cdot)$ represents the divergence operator. Eq. (7) can be linear or nonlinear, depending on the constitutive relations used for the material in consideration and on whether the displacements are small or large [27].

The boundary conditions needed to solve Eq. (7) are,

$$\begin{aligned}\mathbf{u} &= \mathbf{u}_S \quad \text{na } S_u,\\ \tau\cdot\mathbf{n} &= \mathbf{f}^S \quad \text{na } S_f\end{aligned} \tag{8}$$

where S_u and S_f represent the parts of the boundary with prescribed displacements $\mathbf{u}_s$, and tractions $\mathbf{f}^S$, respectively. $\mathbf{n}$ is a unit outward normal vector to the boundary.

C. Fluid Flow Equations

The equations of motion of a compressible Newtonian fluid flow in the ALE description of motion are

$$\rho\frac{\delta\mathbf{v}}{\delta t}+\rho\left[(\mathbf{v}-\hat{\mathbf{v}})\cdot\nabla\right]\mathbf{v}=\nabla\cdot\tau+\mathbf{f}^B \tag{9}$$

$$\frac{\delta\rho}{\delta t}+(\mathbf{v}-\hat{\mathbf{v}})\cdot\nabla\rho+\rho\nabla\cdot\nabla=0 \tag{10}$$

$$\rho\frac{\delta e}{\delta t}+\rho(\mathbf{v}-\hat{\mathbf{v}})\cdot\nabla e=\psi D-\nabla\cdot\mathbf{q}+q^B \tag{11}$$

where ρ is the fluid density, $\delta/\delta t$ is the total time derivative "seen" by a probe moving with the ALE frame, $\mathbf{v}$ is the fluid velocity, $\hat{\mathbf{v}}$ is the velocity of the moving ALE frame, τ is the fluid stress tensor, $\mathbf{f}^B$ represents the vector of fluid body forces, e is the specific internal energy, $\mathbf{D}$ is the velocity strain tensor, $2\mathbf{D}=\nabla\mathbf{v}+(\nabla\mathbf{v})^T$, $\mathbf{q}$ is the heat flux vector, q^B is the rate of heat generated pre unit volume, $(\nabla\cdot)$ and (∇) represent the divergence and gradient operators respectively and $(\cdot)$ indicates internal product [20-21].

The constitutive relations for a Newtonian fluid are

$$\tau=\left[-p+\lambda\nabla\cdot\mathbf{v}\right]\mathbf{I}+2\mu\mathbf{D}, \tag{12}$$

where p is the fluid pressure, $\mathbf{I}$ is the identity tensor, μ and λ are the first and second coefficients of viscosity. For a wide variety of conditions the Stokes hypothesis $\lambda=-2\mu/3$ accurately describes the behavior of the fluid flow and therefore it is generally used [9,27].

The constitutive equations for head transfer inside the body are $\mathbf{q}$ = -$\mathbf{k}$ $\nabla\theta$, where $\mathbf{k}$ is the conductivity tensor and θ is the temperature. The state equation are $\rho=\rho(p,\theta)$ and $e=e(p,\theta)$ [23,26].

Note that in the case of an incompressible fluid, the density is not a function of time and eq. (10) reduces to $\nabla\cdot\mathbf{v}=0$. The Euler equations of motion are used when the fluid viscosity is neglected in the model.

Dynamic equilibrium of fluid domain involving effect of moving mesh describes modified Navier-Stokes equations. Let us to assume temperature independent problem.

Together with traditional boundary conditions defined for fluid domain (pressure and velocity), additional special conditions are considered:

- free surface, the interface between fluid and gas,
- FSI boundary, common boundary between solid and fluid.

D. Fluid Domain, Free Surface, Boundary conditions

Moving boundaries, free surface can be considered when employing the ALE formulation for the fluid flow equations. In case of moving boundaries, the condition that must be satisfied are $\hat{\mathbf{u}}\cdot\mathbf{n}=\hat{u}_s$ and $\hat{\mathbf{u}}\cdot\mathbf{t}=\hat{u}_t$, where $S_{\hat{u}}.S_{\hat{u}}$ corresponds to the part of the surface with imposed displacements $\hat{u}_s$ and $\hat{u}_t$ in the normal and tangential directions respectively, $\mathbf{n}$ and $\mathbf{t}$ are unit normal and tangent vectors to the boundary and $\hat{\mathbf{u}}$ is the boundary displacement [22,28].

When free surface is considered, the effect of air is usually included only as a pressure p_0

$$-p_0\mathbf{n}\text{-}\cdot\tau\cdot\mathbf{n}\,\tau=\alpha\left(\frac{1}{R_t}+\frac{1}{R_s}\right)\mathbf{n}, \tag{13}$$

where τ is stress tensor, $\mathbf{n}$ is a unit normal vector to the interface surface pointing outwards of free surface, α is the coefficient of surface tension between the fluid and air and R_t and R_s are the principal radii of curvatures of interface surface.

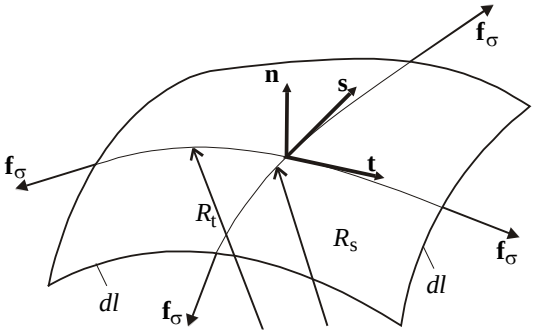

Fig. 2 element of free surface - the interface between fluid and gas

Assume that the surface at a reference time t_0 is represented by the function $S({}^0\mathbf{x},\mathbf{t}_0)=0$, where ${}^0\mathbf{x}$ is the vector of coordinates of the particles that are located on the free surface at time t_0. The following condition must be satisfied

$$\frac{\delta\mathbf{S}}{\delta\mathbf{t}}+(\mathbf{v}-\hat{\mathbf{v}})\cdot\nabla S=\mathbf{0}, \tag{14}$$

which ensures that the particles, that are at the free surface at time t_0, will remain on that surface for all times.

Dynamic boundary condition for free surface express balance of forces between interactive forces of liquid and gas

$$\begin{aligned}\mathbf{f}_l.\mathbf{n}+\sigma K &= -\mathbf{f}_g\ \mathbf{n},\\ \mathbf{f}_l.\mathbf{t}+\sigma K &= -\mathbf{f}_g\ \mathbf{t},\\ \mathbf{f}_l.\mathbf{s}+\sigma K &= -\mathbf{f}_g\ \mathbf{s}.\end{aligned} \tag{15}$$

where $\mathbf{f}_l$ resp. $\mathbf{f}_g$ are forces exerted by *liquid*, resp. *gas*, $\mathbf{t}$ a $\mathbf{n}$ tangent and normal to free surface and $\mathbf{s}$ is surface tension (if present) [19,22].

Kinematic boundary condition states that the velocity at a point of free surface moves together with point of FE-mesh. Thus

$$(\mathbf{v}-\mathbf{v}_b).\mathbf{n}=0. \tag{16}$$

For every point on surface are given conditions in normal

direction **n** and in two tangent directions **t** and **s** to surface of free surface:

E. Interface Between Fluid Flow and Solid

For a problem of a viscous fluid flow that is interacting with a solid medium, equilibrium and compatibility, conditions must be satisfied at the fluid-structure interface.

The conditions are

$$\tau^S \cdot \mathbf{n} = \tau^F \cdot \mathbf{n}, \tag{17}$$

$$\mathbf{u}^I(t) = \hat{\mathbf{u}}(t)$$

$$\dot{\mathbf{u}}^I(t) = \mathbf{v}^I(t) = \hat{\mathbf{v}}^I(t), \tag{18}$$

$$\ddot{\mathbf{u}}^I(t) = \dot{\mathbf{v}}^I(t) = \dot{\hat{\mathbf{v}}}^I(t)$$

where **n** is unit vector normal to the fluid-solid interface, **u** a $\hat{\mathbf{u}}$ are the displacements of the structure and fluid domain, **v** is the fluid velocity and $\hat{\mathbf{v}}$ the velocity of the fluid domain. The dot represents a time derivative, and the supetscripts *I*, *S* a *F* denote interface and the solid and fluid media respectively [3,24].

Kinematic boundary condition assumes velocities and displacements of FSI boundary are represented in Fig. 2. Indexes *f*, resp. *s* mean fluid, resp. solid.

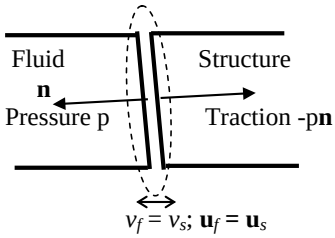

Fig. 3 common velocity and displacement of FSI boundary

F. Finite Elements Discretization

Any of unknown physical variables in Finite element method are expressed in terms of nodal values instead of field value. That causes local discontinuity of the problem, but globally, with regards to whole FE model all governing equations are satisfied.

Unknown variables (displacement, velocity and pressure) are approximated using so called shape functions N.

$$\hat{\mathbf{u}} = \mathbf{N}\,\mathbf{U}, \quad \hat{\mathbf{v}} = \mathbf{N}\,\mathbf{V}, \quad \hat{\mathbf{p}} = \mathbf{N}\,\mathbf{P}, \tag{19}$$

where **U**, **V**, resp. **P** are nodal values of initially unknown fields, **N** are shape functions.

Applying one of appropriate variation principle, governing equations are transformed into integral form, in which interpolations (13) are being easily incorporated and subsequently proceeded in numerical calculation.

As the governing equations are basically nonlinear and time dependent, an appropriate linearization should be used together with a discretization in time domain. Plenty of methods by linearization and time discretization were published in the past. ADINA has implemented some of most popular of them [29].

G. Structure/Solid Discretized Equation

The linearized discrete equations of a structure/solid medium at time t can be expressed as follows

$$\mathbf{M_u}\mathbf{u} + \mathbf{K_u}\mathbf{u} = \mathbf{R_u} - \mathbf{F_u}, \tag{20}$$

where $\mathbf{M_u}$ and $\mathbf{K_u}$ are the mass matrix and tangent stiffness matrix respectively, **u** is the vector of incremental nodal point displacement, $\mathbf{R_u}$ is the vector of externally applied forces and $\mathbf{F_u}$ contains known terms of the linearization. If the structural response is linear, then the same equations are applicable, except when $\mathbf{F_u}$ is set to zero, **u** corresponds to the vector of total nodal point displacement.

H. Fluid Flow Discretized Equations

For the ALE fluid flow equations of motion, the linearized Navier-Stokes discrete equations can be represented by

$$\left[\mathbf{M}_v\ \hat{\mathbf{M}}_v\right]\begin{bmatrix}\dot{\mathbf{v}}\\ \dot{\hat{\mathbf{v}}}\end{bmatrix} + \left[\mathbf{K}_v\ \hat{\mathbf{K}}_v\right]\begin{bmatrix}\mathbf{v}\\ \hat{\mathbf{u}}\end{bmatrix} = \mathbf{R}_v - \mathbf{F}_v, \tag{21}$$

where $\mathbf{M}_v$ and $\mathbf{K}_v$ are the mass and tangent coefficient matrices of the fluid flow, $\hat{\mathbf{M}}_v$ and $\hat{\mathbf{K}}_v$ are tangent mass and coefficient matrices corresponding to the linearized ALE terms which couple with the mesh movement, where **v** is vector of incremental nodal point velocities, $\hat{\mathbf{u}}$ and $\hat{\mathbf{v}}$ are the vectors of incremental mesh displacements and velocities, $\mathbf{R}_v$ is vector of discretized externally applied forces and $\mathbf{F}_v$ contains known terms from the linearization.

I. Coupled Fluid Flow and Structural Equations

To solve an FSI problem using finite element methods, the discrete Eqs. (20) and (21) can be coupled using the equilibrium and kinematic conditions at the interface. The coupling of the fluid and structural response can be achieved numerically in different ways but in all cases, of course, the conditions of displacement compatibility and traction equilibrium along the structure-fluid interfaces have to be satisfied by displacement compatibility $\mathbf{d_f}=\mathbf{d_s}$ and traction equilibrium $\mathbf{f_f}=\mathbf{f_s}$, where $\mathbf{d_f}$ and $\mathbf{d_s}$ are the displacements and $\mathbf{f_f}$ and $\mathbf{f_s}$ are the tractions of the fluid and solid respectively [2,25].

Using the superscripts *I*, *F*, *S* to indicate fluid/structure interface and interior fluid and structure/solid degrees of freedom respectively and assuming that no external forces are applied at the interfaces, the equilibrium condition (17) can be expressed as

$$\mathbf{R}_u^I + \mathbf{R}_v^I = \mathbf{0} \tag{22}$$

And the compatibility condition (18) is

$$\mathbf{u}^I = \hat{\mathbf{u}}^I$$

$$\dot{\mathbf{u}}^I = \hat{\mathbf{v}}^I = \mathbf{v}^I, \tag{23}$$

$$\ddot{\mathbf{u}}^I = \dot{\mathbf{v}}^I$$

where **u**, $\hat{\mathbf{u}}$ and $\hat{\mathbf{v}}$ are increments in the nodal displacements, mesh displacements and mesh velocities.

The movement of the interior mesh nodes is a function of the movement of the interface nodes. It will be assumed that the effect of the mesh motion is contained in the matrices $\hat{\mathbf{M}}_v$

a $\hat{\mathbf{K}}_v$, than Eqs. (21) is now expressed as

$$\begin{bmatrix} \mathbf{M}_v^{II} & \mathbf{M}_v^{IF} \\ \mathbf{M}_v^{FI} & \mathbf{M}_v^{FF} \end{bmatrix} \begin{bmatrix} \dot{\mathbf{v}}^I \\ \dot{\mathbf{v}}^F \end{bmatrix} + \begin{bmatrix} \mathbf{M}_v^{II} & \hat{\mathbf{M}}_v^{II} & \mathbf{K}_v^{IF} \\ \mathbf{K}_v^{FI} & \hat{\mathbf{M}}_v^{FI} & \mathbf{K}_v^{FF} \end{bmatrix} \begin{bmatrix} \mathbf{v}^I \\ \mathbf{v}^F \end{bmatrix} + \\ + \begin{bmatrix} \hat{\mathbf{K}}_v^{II} & \mathbf{0} \\ \hat{\mathbf{K}}_v^{FI} & \mathbf{0} \end{bmatrix} \begin{bmatrix} \mathbf{u}^I \\ \mathbf{u}^F \end{bmatrix} = \begin{bmatrix} \mathbf{R}_v^I \\ \mathbf{R}_v^F \end{bmatrix} - \begin{bmatrix} \mathbf{F}_v^I \\ \mathbf{F}_v^F \end{bmatrix}, \quad (24)$$

where $\mathbf{u}^F$ corresponds to the vector of increments of internal fluid particle displacements which aren't calculated.

Using (20) and (22) to the coupled FSI equations (24) are given

$$\mathbf{A}\ddot{\mathbf{U}} + \mathbf{B}\dot{\mathbf{U}} + \mathbf{C}\mathbf{U} = \mathbf{G} \quad (25)$$

Eqs. (25) can be written as

$$\begin{bmatrix} \tilde{\mathbf{K}}_u^{SS} & \tilde{\mathbf{K}}_u^{SI} & \mathbf{0} \\ \tilde{\mathbf{K}}_u^{IS} & \tilde{\mathbf{K}}_u^{II} + \tilde{\mathbf{K}}_v^{II} & \tilde{\mathbf{K}}_v^{IF} \\ \mathbf{0} & \hat{\mathbf{K}}_v^{FI} & \hat{\mathbf{K}}_v^{FF} \end{bmatrix} \begin{bmatrix} \mathbf{U}^S \\ \mathbf{U}^I \\ \mathbf{U}^F \end{bmatrix} = \begin{bmatrix} \mathbf{R}_u^S \\ \mathbf{0} \\ \mathbf{R}_v^F \end{bmatrix} - \begin{bmatrix} \tilde{\mathbf{F}}_u^S \\ \tilde{\mathbf{F}}_u^I + \tilde{\mathbf{F}}_v^I \\ \tilde{\mathbf{F}}_v^F \end{bmatrix}, \quad (26)$$

where $\tilde{\tilde{\mathbf{K}}}$ represents the linearized coefficient matrix, $\mathbf{U}$ is the vector of incremental nodal point displacements/velocities, $\mathbf{R}$ is vector of discretized externally applied forces, and the vector $\tilde{\mathbf{F}}$ contains known terms from the linearization and time discretization. $\mathbf{U}^S$ contains displacements, $\mathbf{U}^F$ velocities and in $\mathbf{U}^I$ in general, either velocities or displacements are considered [5,22].

It is frequently convenient to discretize an FSI problem using completely different meshes for each field. Usually, due to the nature of fluid flows, finer meshes are needed for the fluid domain than for discretization of the structure. However, regardless of the meshes employed in the discretization of the fluid and structure, the equilibrium and compatibility conditions, Eqs. (17) and (18), have to be satisfied at the interface. Fluid and solid meshes and mappings of displacements and tractions on fluid-structure interfaces as illustrated in Fig. 4. The solid arrows indicate traction mapping and the dashed arrows indicate displacement mapping.

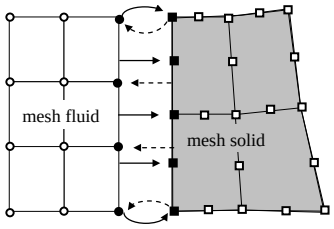

Fig. 4 illustration of fluid and solid meshes and mappings of displacements and tractions on fluid-structure interfaces

The response of the coupled FSI system is calculated using already developed fluid flow and structural solvers. The complete system is divided into subsystems (fluid domain, and structure/solid domain). The solution of one domain is separated from solution of the other domain. Iterations between the domain equations are necessary, at each time or load step, to guarantee convergence of the fully coupled fluid-structure interaction solution. One of the most widely employed FSI portioned schemes is called staggered procedure.

The first step corresponds to the solution of the ALE fluid flow equations using the displacements and velocities of the interface as boundary conditions. Once the results are obtained, traction vectors exerted by the fluid onto the structure are calculated and applied to the structure as force boundary conditions and the structural equations are solved.

$$\mathbf{F} = \int_{S_I} \left(\mathbf{H}^S\right)^T \mathbf{f}_F^I(s)\, ds, \quad (27)$$

where $\mathbf{H}^S$ is the structural finite element displacement interpolation matrix evaluated at the interface, $\mathbf{f}_F^I(s)$ are fluid traction at the interface, where s represents the interface surface. T indicated transpose and S_I refers to the fluid structure. The next step is to solve the fluid flow equations again; but after having used the calculated structural displacements to update the fluid domain and mesh and the velocities of the interface. The procedure is repeated until convergence of the FSI problem is achieved [22,27].

The main advantage of partitioned procedures is that already developed field codes (for the fluid and structure) can be used, and only the transfer of information between them needs to be programmed. The partitioned procedures are most effective in a case when the coupling between the fluid and the structure is weak, because the response of each field is not significantly affected.

IV. Numerical Example

In this study, the ground supported reinforced concrete rectangular tank - endlessly long shipping channel is considered as shown in Fig. 5.

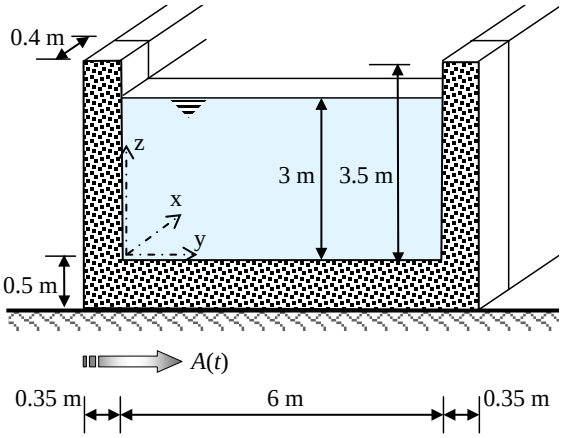

Fig. 5 details of tank geometry

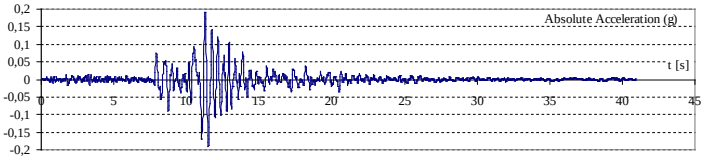

Fig. 6 the accelerogram Loma Prieta, California

The material characteristics of tank are: Young's modulus E = 37 GPa, Poisson ratio ν = 0.20, density ρ = 2550 kg/m^3. There is no roof slab structure covering the channel. The material characteristics of fluid filling (H_2O) are: bulk modulus $B = 2.1 \cdot 10^9$ N/m^2, density ρ_w = 1 000 kg/m^3. As the excitation input, we consider horizontal earthquake load given by the accelerogram of the earthquake in Loma Prieta, California (18.10.1989), Fig. 6. In the analysis we use just the accelerogram for the seismic excitation in y - direction.

Dynamic time-history response of concrete open top rectangular liquid storage tanks - chipping channel was performed by application of Finite Element Method (FEM) utilizing software ADINA. Arbitrary-Lagrangian-Eulerian (ALE) formulation was used for the problem. Two way Fluid-Structure Interaction (FSI) techniques were used for simulation of the interaction between the structure and the fluid at the common boundary. The solid walls and base of the shipping channel was modeled by using 3D SOLID finite element. The fluid inside the shipping channel was modeled by using 3D FLUID finite elements. As the excitation for numerical simulation was considered the input time dependent horizontal displacement measured during the earthquake Loma Prieta in California, Fig. 7.

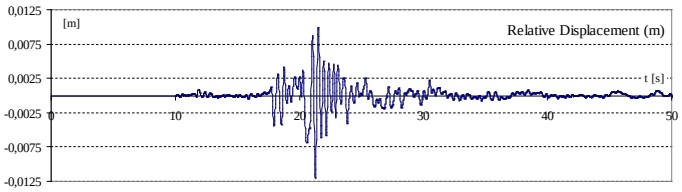

Fig. 7 input time dependent horizontal displacement measured during of earthquake Loma Prieta

FE-Models for 3D FSI analysis of endlessly long shipping channel were documented in Fig. 8a and Fig. 8b. Fig. 8a shows the solid domain where FSI boundary is showing black color and Fig. 8b fluid domain.

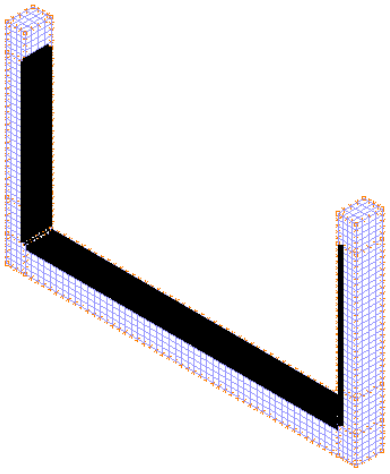

Fig. 8a FE-Model of the solid domain for 3D FSI analysis

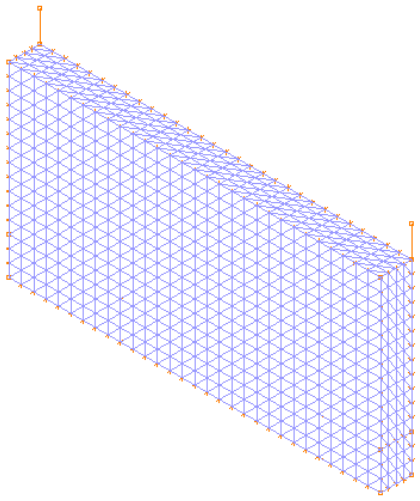

Fig. 8b FE-Model of fluid domain for 3D FSI analysis

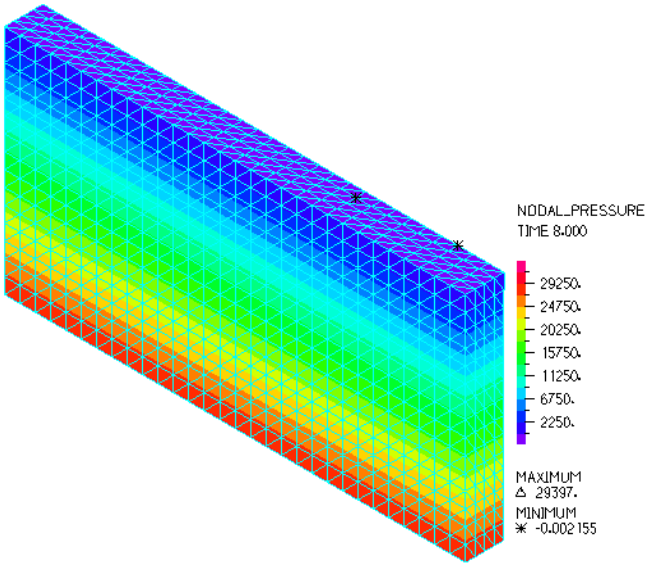

Fig. 9 pressure of fluid in time 8 s

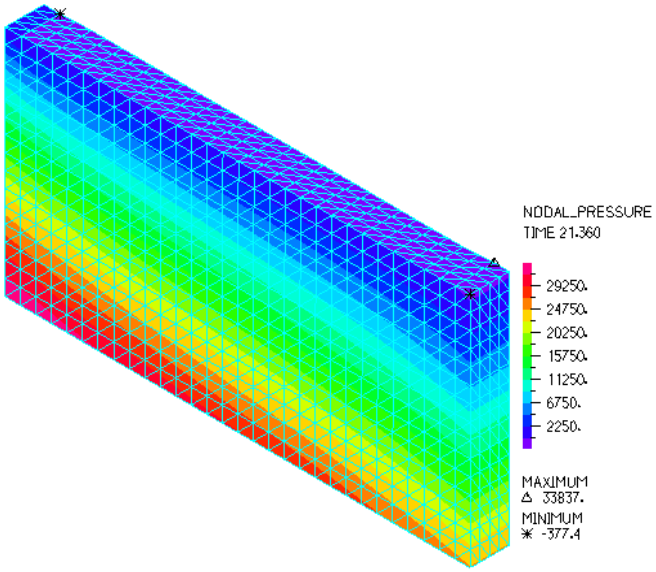

Fig. 10 pressure of fluid in time 21.36 s

The Fig. 9 and Fig. 10 present:

- fluid pressure distribution in quiet condition, in time 8.0 s, (before the earthquake) when only gravity load is applied to the fluid domain.
- fluid pressure distribution in time of the peak response of fluid pressure, in time 21.36 s.

The resulting time dependent response of the pressure of fluid was described in Fig. 11 and Fig. 12, Fig. 11 in point ”DL” (Down Left edge of fluid region) and Fig. 12 in point ”DR” (Down Right edge of fluid region). We can see that the time dependent response of the fluid pressure in ”DL” and ”DR” points are almost asymmetric.

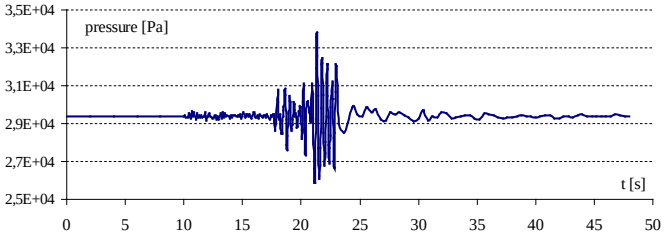

Fig. 11 time dependent response of the fluid pressure in “DL” point

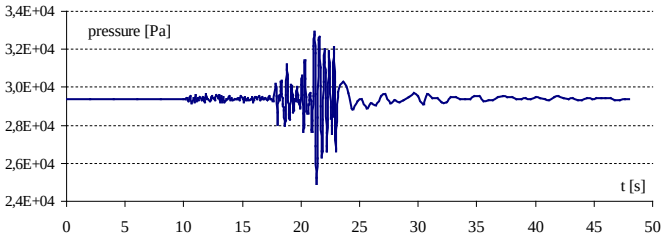

Fig. 12 time dependent response of the fluid pressure in “DR” point

Fig. 13 shows the comparison of resulting time dependent responses of the fluid pressure within time interval 17-27 s in points ”DL”, ”DR” and ”DM” (Down Middle of fluid region). Only the time dependent response of the fluid pressure within time interval 17-27 s in point ”DM” is described in Fig. 14.

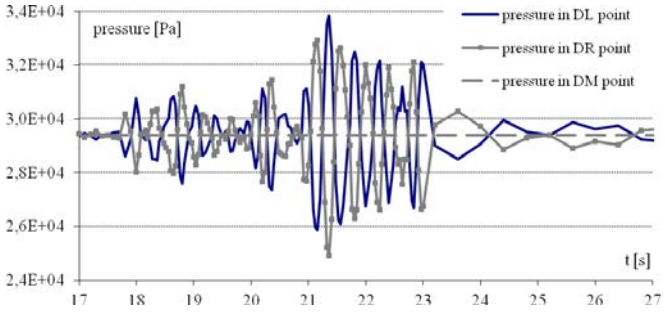

Fig. 13 time dependent response of the fluid pressure in “DR”, “DL” and “DM” points

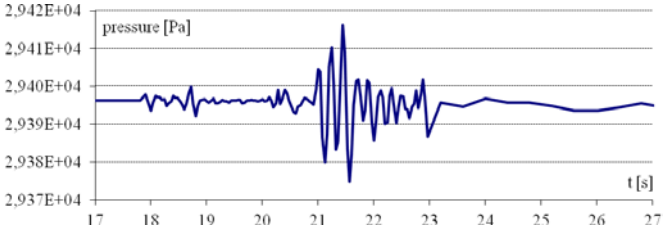

Fig. 14 time dependent response of the fluid pressure in “DM” point

The Fig. 15 shows the shape of fluid domain and vertical displacement distribution in time 21.56 s, it is the time when peak response of vertical displacement was obtained.

The timing of the peak response correlates well with peak excitation (Loma Prieta as in Fig. 6), which the numerical analysis makes realistic enough.

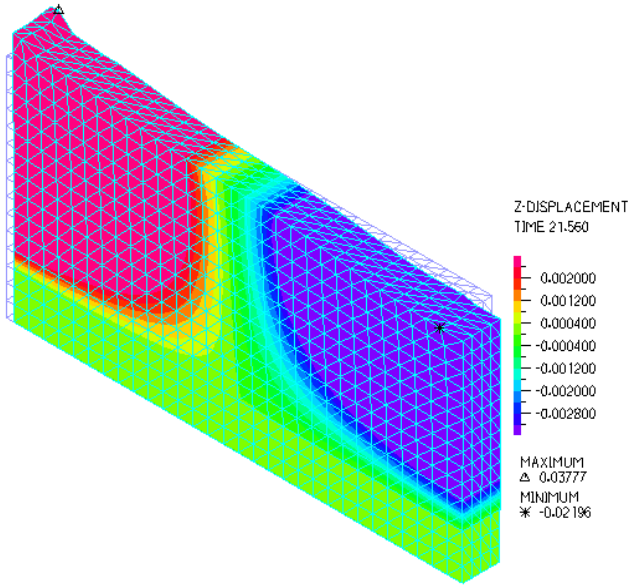

Fig. 15 shape of fluid domain and vertical displacement of fluid in time 21.56 s

The resulting time dependent vertical displacement of fluid in the point ”UL” (Up Left edge of fluid region on free surface) was presented in Fig. 16, whereas the same response of fluid in point ”UR” (Up Right edge of fluid region on free surface) was shown in Fig. 17.

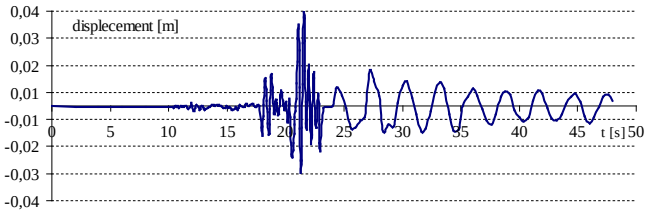

Fig. 16 time dependent response of the vertical displacement of fluid in “UL” point

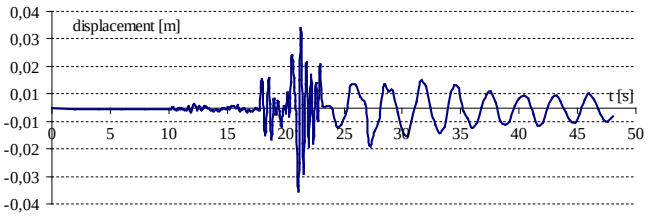

Fig. 17 time dependent response of the vertical displacement of fluid in “UR” point

Fig. 18 shows the comparison of resulting time dependent responses of the fluid vertical displacement within time interval 17-27 s in points ”UL”, ”UR” and ”UM” (Up Middle of fluid region on free surface). It is seen that vertical displacement distribution in ”DL” and ”DR” points are almost asymmetric.

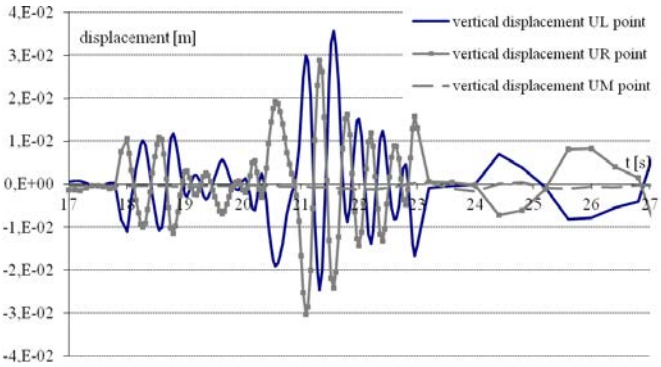

Fig. 18 time dependent response of the vertical displacement of fluid in “UL”, “UR” and “UM” points

Only the resulting time dependent response of the fluid vertical displacement within time interval 17-27 s in point ”DM” is in Fig. 19.

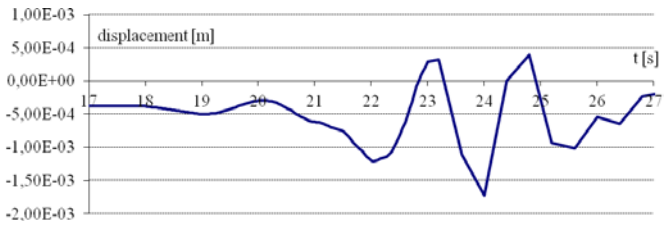

Fig. 19 time dependent response of the vertical displacement of fluid in “UM” point

The resulting time dependent horizontal and vertical displacements of fluid within time interval 17-30 s in point ”UL” together are documented in Fig. 20, while the same responses of fluid are shown in “UR” point in Fig. 21.

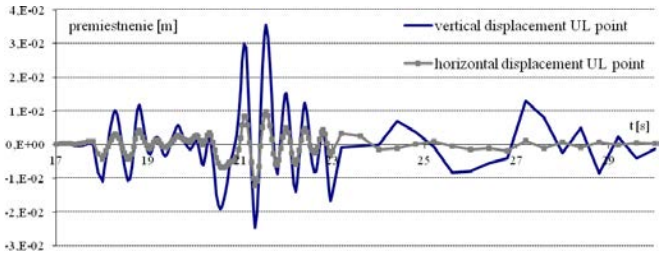

Fig. 20 time dependent response of the vertical and horizontal displacement of fluid in “UL” point

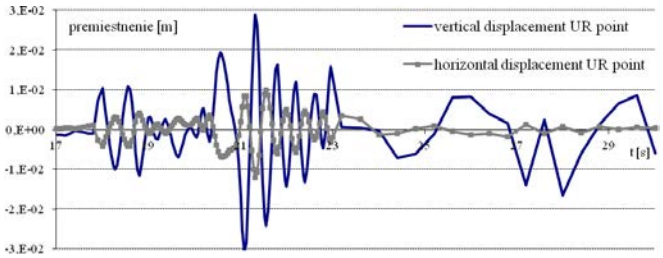

Fig. 21 time dependent response of the vertical and horizontal displacement of fluid in “UR” point

Fig. 22 and Fig. 23 give the shape of fluid domain and velocity distribution in time 21.44 s - the time of peak values of velocities:

- Fig. 22 shows horizontal velocity distribution,
- Fig. 23 vertical velocity distribution.

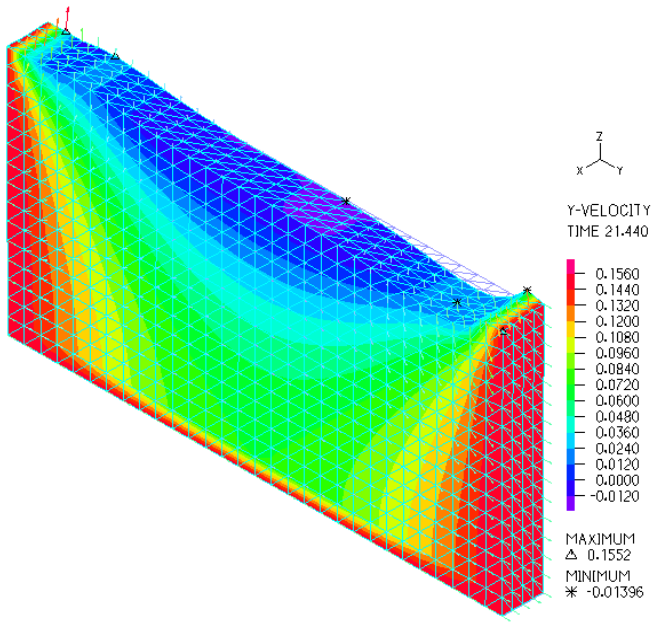

Fig. 22 shape of fluid domain and horizontal velocity in time 21.44 s

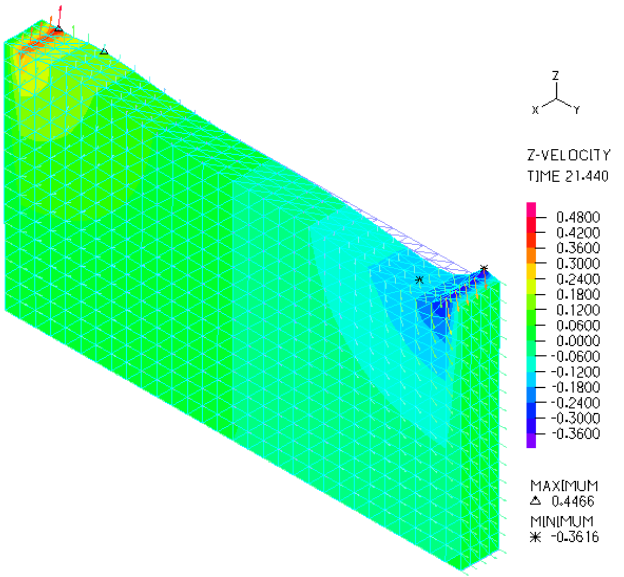

Fig. 23 shape of fluid domain and vertical velocity in time 21.44 s

The Fig. 24 documents deformed shape of shipping channel and Von Mises stress distribution over the domain of interest in time t = 21.44 s, it is the time when peak response was obtained.

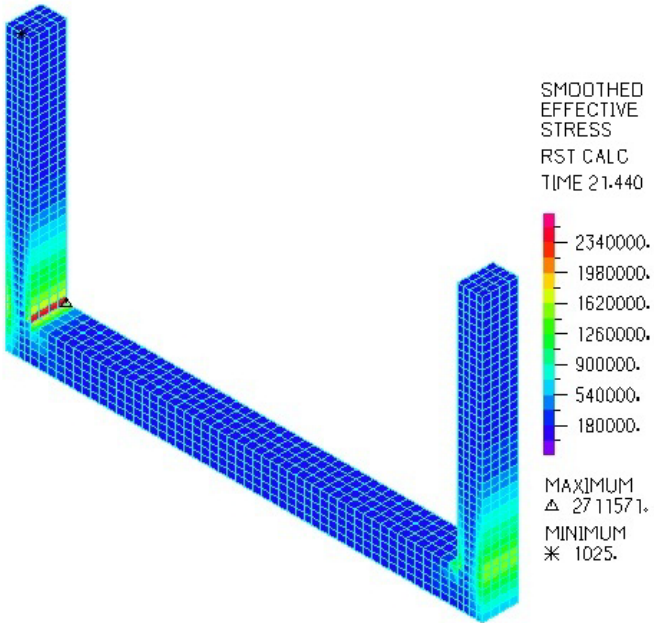

Fig. 24 shape and Von Mises stress of tank in time t = 21.44 s

The time dependent relative horizontal displacement of the tank's up corner to down corner was presented in Fig. 25 on the left wall, whereas the same response of fluid on the right wall in Fig. 26. Fig. 27 and Fig. 28 show the time dependent of the same tank responses within time interval 17-27 s, Fig. 27 on left side and Fig. 28 on the right side.

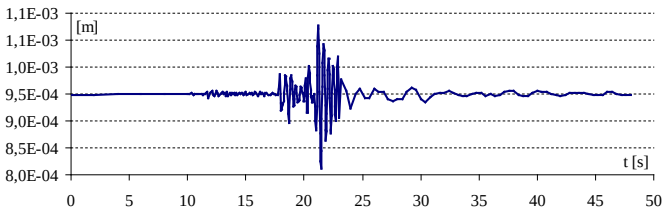

Fig. 25 time dependent response of tank relative horizontal displacement on the left wall

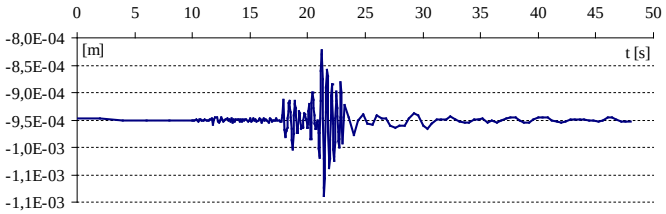

Fig. 26 time dependent response of tank relative horizontal displacement on the right wall

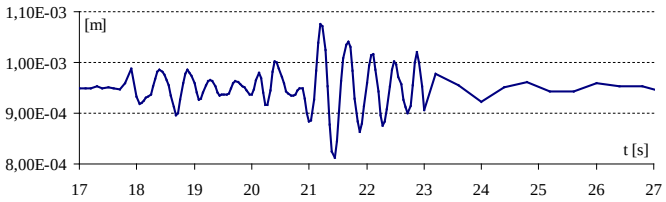

Fig. 27 time dependent response of tank relative horizontal displacement on the left wall within time interval 17-27 s

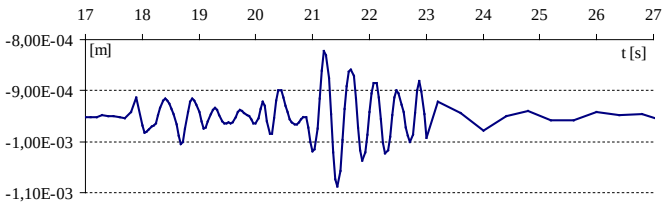

Fig. 28 time dependent response of tank relative horizontal displacement on the right wall within time interval 17-27 s

V. Concluding Remarks

The ground supported rectangular endlessly long open top shipping channel was analyzed using the FEM, ALE, FSI formulation. The channel was excited by the time dependent horizontal displacement measured during the earthquake Loma Prieta in California. Basic responses of the interest were: pressure and displacement of fluid domain and structural deformation and stress distribution over the tank.

The maximum pressure acting on the wall is located at the bottom of the tank. The maximum value of hydrostatic pressure using numeric simulation FEM ALE FSI is 29397 Pa,

it correlates with analytical result of hydrostatic pressure: $p = \rho \cdot g \cdot h = 1000 \cdot 9.81 \cdot 3.0 = 29430$ Pa.

The peak results of fluid domain given by numerical simulation FEM ALE FSI are: fluid pressure: 33.837 kPa in time 21.36 s on the left wall, fluid vertical displacement: 3.77 cm in time 21.56 s in left part of free surface, vertical velocity of fluid: 0.1552 ms^{-1} in time 21.44 s in left part of fluid domain.

The peak hydrodynamic pressure and vertical displacement of fluid in the shipping channel along left side wall were similar, asymmetric and with a little higher values as along the right wall.

The peak results of solid domain obtained using numerical simulation FEM ALE FSI are: relative horizontal displacement of container wall: 1.074 mm, Von Mises stress of tank: 2.7 MPa in time 21.44 s.

ACKNOWLEDGMENT

This work was supported by the Scientific Grant Agency of the Ministry of Education of Slovak Republic and the Slovak Academy of Sciences the project VEGA 1/0477/15 "Numerical analysis and modeling of interactive problems in multilayered composite structural members".

REFERENCES

[1] G. K. Batchelor, An introduction to fluid dynamics. Cambridge: Cambridge University Press. 1967.

[2] Bathe, K., J., Zhang, H., ji, S., 1999: Finite Element Analysis of fluid Flows with structural interactions. In: Computer & Structures, Vol.72, No. 2/2, s. 1-16. 1999.

[3] Bathe, K., J., Zhang, H., Wang, M., H., 1995: Finite Element Analysis of incompressible and compressible fluid Flows with free surfaces and structural interaction. In: Computer & Structures, Vol.56, No. 2/2, s. 193-213. 1995.

[4] Bathe, K., J., Zhang, H., 2004: Finite Element developments for general fluid flows with structural interaction. In: International journal for numerical methods in engineering, 2004.

[5] A. Di Carluccio, G. Fabbrocino, E. Salzano, G. Manfredi, Analysis of pressurized horizontal vessels under seismic excitation. In: ICSV18: 18th The World Conference on Earthquake Engineering: October 12 – 17, 2008, Beijing, China.

[6] A. H. N. Chegini, G. Pender, Determination of Small Size Bedload Sediment Transport and its Related Bedform under Different Uniform Flow Conditions. In: WSEAS Transactions on Environment and Development. Vol. 8 (4), 2012, pp. 158-167.

[7] G. B. Jacobs, W. S. Don, T. Dittmann, High-order resolution Eulerian–Lagrangian simulations of particle dispersion in the accelerated flow behind a moving shock, In: Theoretical and Computational Fluid Dynamics, ISSN 0935-4964, January 2012, Volume 26, Issue 1, pp 37-50

[8] N. Jendzelovsky, N., L. Balaz, Numerical Modeling of Cylindrical Tank and Compare with Experiment. In: Applied Mechanics and Materials. ISSN 1660-9336. 2014, Vol. 617, pp. 148-151.

[9] N. Jendzelovsky, N., L. Balaz, Modeling of a gravel base under the cylindrical tank. In: Advanced Materials Research. Vol. 969, pp. 249-252. ISSN 1022-6680.

[10] E. Kock, L. Olson, Fluid-structure interaction analysis by the finite element method a variational approach. In: International Journal for Numerical Methods in Engineering. Volume 31, Issue 3, pp. 463-491, March 1991, John Wiley & Sons, Ltd.

[11] K. Kralik, J. Kralik jr., Probability assessment of analysis of high-rise buildings seismic resistance, Advanced Materials Research, Volume 712-715, 2013, pp. 929-936.

[12] K. Kralik, J. Kralik jr., Seismic analysis of reinforced concrete frame-wall systems considering ductility effects in accordance to Eurocode. In: Engineering Structures. 2009. P. 2865-2872. ISSN 0141-029.

[13] M. Krejsa, P. Janas, V. Krejsa, Software application of the DOProC method. In: International Journal of Mathematics and Computers in Simulation Vol. 8, No. 1 (2014), pp. 121-126 ISSN: 1998-0159.

[14] K. Kotrasova, Sloshing of Liquid in Rectangular Tank. In: Advanced Materials Research. No. 969 (2014), p. 320-323. - ISBN 978-303835147-4, ISSN 1662-8985.

[15] K. Kotrasova, I. Grajciar, Dynamic Analysis of Liquid Storage Cylindrical Tanks Due to Earthquake. In: Advanced Materials Research. No. 969 (2014), pp. 119-124. - ISBN 978-303835147-4, ISSN 1662-8985.

[16] K. Kotrasova, I. Grajciar, E. Kormanikova, Dynamic Time-History Response of cylindrical tank considering fluid - structure interaction due to earthquake. Transport Structures and Wind Engineering. In: Applied Mechanics and Materials. No. 617 (2014), pp. 66-69, ISSN 1660-9336.

[17] K. Kotrasova, I. Grajciar, E. Kormanikova, A Case Study on the Seismic Behavior of Tanks Considering Soil-Structure-Fluid Interaction. In: Journal of vibration engineering & technologies. ISSN 2321-3558, Vol. 3, Issue 3, p. 315-330.

[18] K. Kotrasová, E. Kormaníková, S. Leoveanu, Seismic analysis of elevated reservoirs. In: SGEM 2013: 13th International Multidisciplinary Scientific Geoconference: Water resources, forest, marine and ocean ecosystems : conference proceedings: 2013, P. 293-300. ISSN 1314-2704.

[19] I. S. Leoveanu, K. Kotrasová, E. Kormaníková, Using of computer fluid dynamics in simulation of the waste reservoirs processes. In: Advanced Materials Research. No. 969, 2014, p. 351-354. ISSN 1662-8985.

[20] . S. Leoveanu, K. Kotrasová, E. Kormaníková, Using of computer fluid dynamics in simulation of the waste reservoirs processes. No. 969. 2014, p. 351-354. ISSN 1662-8985.

[21] I. S. Leoveanu, D. Taus, K. Kotrasová, E. Kormaníková, Fluid seismic modelling inside reservoirs walls and shipping channel based on transport phenomena. In: Proceedings of the 13th WSEAS international conference on Automatic control, modelling & simulation (WSEAS), 2011. P. 398-403. ISSN 2223-2907.

[22] H. Lamb, Hydrodynamics. 6th ed New York, Dover Publications; 1945.

[23] J. Melcer, Dynamic response of a bridge due to moving loads, Journal of Vibrational Engineering and Technologies, vibration engineering & technologies. ISSN 2321-3558, Volume 3, Issue 2, 1 January 2015, Pages 199-209.

[24] S. Rugonyi, K., J., Bathe,: On Finite Element Analysis of Fluid Coupled with Structural Interaction. In: CMES, vol. 2, no. 2, s. 195-212, 2001.

[25] M. Safari, Analytical Solution of Two Model Equations for Shallow Water Waves and their Extended Model Equations by Adomian's Decomposition and He's Variational Iteration Methods. In: WSEAS Transactions on Mathematics. ISSN: 1109-2769, Vol. 12 (1), 2013, pp. 1-16.

[26] E. Sávio De Góes Maciel: TVD and ENO Applications to Supersonic Flows in 3D – Part II, In: WSEAS Transactions on Fluid Mechanics, ISSN 1790-5087, Vol. 8 (1), 2013.

[27] O. Sucharda, J. Brozovsky, Bearing capacity analysis of reinforced concrete beams, International Journal of Mechanics, Volume 7, Issue 3, 192-200, 2013.

[28] V. Michalcova, S. Kuznetsov, S. Pospisil, Numerical and experimental study of the load of an object due to the effects of a flow field in the atmospheric boundary layer. In: International Journal of Mathematics and Computers in Simulation. 2014. 8 (1), pp. 135-140. ISSN 1998-0159

[29] X. Wang, Fundamentals of Fluid – Solid Interactions. Analytical and Computational Approaches. Eselvier, Linacre House, Oxford OX2 8DO, UK, ISSN 157-6917. 2008.

[30] M. Zmindak, I. Grajciar, Simulation of the aquaplane problem. Computers and Structures. Vol. 64, Issue 5-6, September 1997, pp. 1155-1164.

[31] Manual ADINA. 71 Elton Ave, Watertown, MA 02472, USA, ADINA R&D, Inc., October 2005.

[32] Eurocode 8 – Design of structure for earthquake resistance – Part. 4: Silos, tanks and pipelines. January 2006.

K. Kotrasova graduated at the Technical University of Košice, Civil Engineering Faculty, study program - Building Construction. After finishing of the university she started to work at RCC in Spišská Nová Ves as designer and then at the Technical University of Košice, Civil Engineering Faculty, Department of Structural Mechanics. PhD. graduated at the Technical University of Košice, Faculty of Mechanical Engineering, study in program Applied Mechanics. Associate professor graduated at the Technical University of Košice, Civil Engineering Faculty in study program Theory and Design of Engineering Structures. The research topics: seismic analysis of interaction problems: fluid – solid – subsoil, seismic design of liquid storage ground-supported tanks, design of structural elements and structures made of composite materials.

E. Kormanikova graduated at the Technical University of Košice, Civil Engineering Faculty, study program - Building Construction. After finishing of the university she started to work at the Technical University of Košice, Civil Engineering Faculty, Department of Structural Mechanics as assistant. PhD. graduated at the Technical University of Košice, Faculty of Mechanical Engineering, study program - Applied Mechanics. Since 2009 she has worked at Civil Engineering Faculty TUKE, study program - Theory and Design of Engineering Structures, as associate professor. Her research topic is design and optimization of structural elements and structures made of composite materials and seismic analysis of interaction problems: fluid – solid - soil.